(INVITED) Revisiting Duffy's model for Sb3+ and Bi3+ in double halide perovskites: Emergence of a descriptor for machine learning

Philippe Boutinaud

Version of Record: https://www.sciencedirect.com/science/article/pii/S2590147821000127
Manuscript_ae8fda958288b43599661bc8dd5823fb

Revisiting Duffy's model for Sb^{3+} and Bi^{3+} in double halide perovskites: emergence of a descriptor for machine learning

Philippe Boutinaud

Université Clermont Auvergne, Clermont Auvergne INP, CNRS, ICCF, F-63000 Clermont–Ferrand, France

philippe.boutinaud@sigma-clermont.fr

Abstract

The Duffy's model is reformulated for Sb^{3+} and Bi^{3+} in cubic chloro- and bromo-elpasolites with « 0D » perovskite structure. The new equation allows calculating the energy of the first $s^2 \rightarrow s^1p^1$ electron transition from crystal structure data. The Stokes shift pertaining to the Sb^{3+} emission in $Cs_2B^IM^{III}Cl_6$ double perovskites is rationalized based on Waber-Cromer orbital radii, in the approximation of the symmetrically breathing quasi-molecular $(SbCl_6)^{3-}$ octahedron. This constitutes a preliminary structure-property descriptor to be implemented in machine learning algorithms for further computer-assisted design of double halide perovskites doped with Sb^{3+}.

Keywords : Antimony, double halide perovskite, nephelauxetic function, Stokes shift

1. Introduction

Understanding how phosphors work was the essence of George Blasse's research life. This resulted in more than 700 scientific papers and reviews in which solid state spectroscopists are used find answers to their questions. The present report will confirm this statement once more. Several of George Blasse's papers deal with mercury-like cations, i. e. cations with ns^2 electron configuration like Tl^+, Sn^{2+}, Pb^{2+}, As^{3+}, Sb^{3+} or Bi^{3+}. This is not surprising as regard to the attractive attributes of these cations in terms of quantum efficiency and color tunability. However, despite decades of efforts, the spectroscopy of these ions still present shaded areas [1]. We will focus here on Sb^{3+}, a cation that had its glory days in the apatite $Ca_5(PO_4)_3(F,Cl)_2$:Sb^{3+} :Mn^{2+} [2] before being nearly forgotten with the progress of lamp technology. Nevertheless, Sb^{3+} has recently experienced a revival as a dopant in double halide perovskites (DHPs) $A^I_2B^IM^{III}X_6$ (A^I = Cs, Rb, NH_4, etc… ; B^I = Na, K, Ag, etc…; M^{III} = Bi, Sb, Ga, In, etc… and X = Cl, Br) where it shows efficient luminescence [3-11]. This opens new perspectives for this cation and justifies some additional work on its spectroscopy. Besides their applicative interest, DHPs have an ideal cubic elpasolite structure that incorporates ns^2 cations in octahedral halide field without need of charge compensation. Also referred to as « 0D » perovskites - in the sense that the $(MX_6)^{3-}$ octahedra are not interconnected but bridged by $(B^ICl_6)^{5-}$ octahedra and large inorganic (or even larger organic) cations A^I - they form model systems for studying the spectroscopic behavior of localized emitters (Fig. 1).

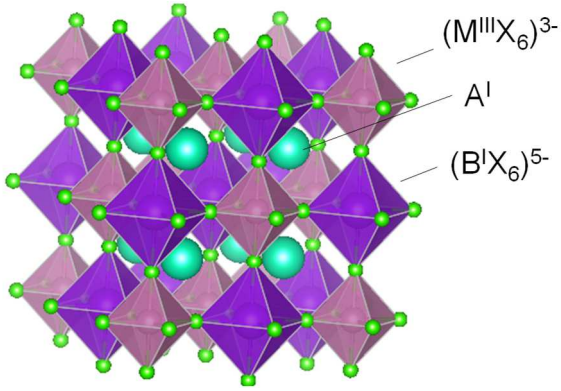

Fig. 1 View of the $A^I_2B^IM^{III}X_6$ double perovskite structure.

The ground and first excited states of Sb^{3+} and Bi^{3+} belong to s^2 and s^1p^1 electron configurations, respectively. In octahedral field, this raises the excited terms $^3A_{1u}$, $^3T_{1u}$, $^3T_{2u}$ and $^1T_{1u}$ in order of increasing energy. The ground state is the spin singlet $^1A_{1g}$ [12]. $^3T_{1u}$ acquires a certain amount of spin singlet character by spin-orbit coupling with the upper lying $^1T_{1u}$ state, which renders the $^1A_{1g} \rightarrow {}^3T_{1u}$ transitions partially allowed. The corresponding absorption/excitation band, labbeled A, is the subject of interest here. This band appears sometimes splitted by the Jahn-Teller (JT) effect. We know that the energy E_A of this transition is lowered as the covalency of the Sb-ligand bond is reinforced. This is expressed by the equation introduced by Duffy and Igram that connects E_A with the nephelauxetic ratio *h* of the host lattice according to [13,14] :

$$E_A = E_f\,(1 - mh) \qquad (1)$$

where E_f is the energy of the A transition in correspondance with *h* = 0, i. e. the free ion. E_f amounts 8.27 eV for Sb^{3+} and 9.41 eV for Bi^{3+} [15]. *h* expresses the ability for a particular ligand to bring about orbital expansion of the central ion and *m* is a measure of the extent to which the s and p orbitals of the central ns^2 ion are expanded by different ligands. It is assumed that *h* relates to the host lattice and depend only upon the anions while *m* depends only upon the cations. For chloride, bromide and iodide the values of *h*, as determined earlier by C. K. Jørgensen from spectroscopic data of transition metal ions [16], are assumed to be fixed at about 2.0, 2.3 and 2.7 respectively. These values statisfactorily reproduce the trends along the nephelauxetic sequence F, Cl, Br, I in ns^2 halides and ns^2-doped

alkali halides [17] and yield *m* values of 0.24 and 0.28 for Sb^{3+} and Bi^{3+}, respectively. In oxidic media, the *m* values are lowered to 0.18 (Sb^{3+}) and 0.21 (Bi^{3+}) but the energy E_f in Eqn. (1) is found 1.82 to 2.47 eV below the tabulated free ions values [14,18]. In the present paper, we show that the (*m,h*) values do not accurately reproduce the optical data of Sb^{3+} or Bi^{3+} in DHPs. We therefore investigate the possibility to reformulate Eqn. (1) by substituting *h* to a more accurate nephelauxetic function, *he*, computable from the crystal structure of the halide lattice. Additionally, the Stokes shifts pertaining to the $^3T_{1u}$ ($^3P_1$) → $^1A_{1g}$ ($^1S_0$) emission of Sb^{3+} in these cubic halide elpasolites is tentatively rationalized in the approximation of symmetrically- breathing $(SbX_6)^{3-}$ octahedron (X=Cl,Br) and based on Waber-Cromer orbital radii that were utilized earlier by G. Blasse and A. Bril [19]. Double perosvkites $A^I_2B^IM^{III}X_6$ constitute a vast family with hundreds of stable chemical compositions that can conveniently be screened by applying machine learning methodologies [20,21]. It is hoped that the preliminary results presented in this work could open perspectives in terms of computer-assisted design strategies of Sb^{3+}-doped DHPs.

2. Method

The new nephelauxetic function *he* of interest is calculated at a given site M(*i*) of the host lattice as follows :

$$he(M(i)) = \sqrt{\sum_1^{N_{M(i)}} f_{c(M(i)-X(i))}\alpha_{(M(i)-X(i))}Q^2_{X(i)}} \quad (2)$$

where $f_{c(M(i)-X(i))}$ and $\alpha_{(M(i)-X(i))}$ represent respectively the fractional covalency and the volume polarization of each chemical bond separating cation M(*i*) to its nearest ligands X(*i*) in binary units to which the host lattice must initially be decomposed [22,23]. The sum runs on the coordination number $N_{M(i)}$ of atom M(*i*). Following the decomposition procedure, a lattice with general formula $A_aB_bM_mX_x$ is first written as $A(i)_{a_i}B(i)_{b_i}M(i)_{m_i}X(i)_{x_i}$ where the index *i* corresponds to the 1, 2, …n crystallographic sites that are occupied by the cations and anions in the crystal structure. We have $a_i = w_i(A)/Z,\ b_i = w_i(B)/Z,\ m_i = w_i(M)/Z,\ x_i = w_i(X)/Z,$ with $w_i(A)$, $w_i(B)$, $w_i(M)$, $w_i(X)$ the multiplicity of the different Wyckoff sites (*i*) occupied by atoms A, B, M and X, and *Z* the number of formula units per unit cell. We have also $\sum_{i=1}^n a_i = a, \sum_{i=1}^n b_i = b, \sum_{i=1}^n m_i = m, \sum_{i=1}^n x_i = x.$

The compound $A(i)_{a_i}B(i)_{b_i}M(i)_{m_i}X(i)_{x_i}$ is then decomposed into binary units consisting of cations A(*i*), B(*i*) and M(*i*) surrounded by $N_{A(i)}$, $N_{B(i)}$ and $N_{M(i)}$ ligands X(*i*), respectively as:

$$\left(A(i)a_i\frac{N_{A(i)-X(i)}}{N_{A(i)}}X(i)x_i\frac{N_{X(i)-A(i)}}{N_{X(i)}}\right)\left(B(i)b_i\frac{N_{B(i)-X(i)}}{N_{B(i)}}X(i)x_i\frac{N_{X(i)-B(i)}}{N_{X(i)}}\right)\left(M(i)m_i\frac{N_{M(i)-X(i)}}{N_{M(i)}}X(i)x_i\frac{N_{X(i)-M(i)}}{N_{X(i)}}\right)$$

The quantities $N_{A(i)-X(i)}$, $N_{B(i)-X(i)}$ and $N_{M(i)-X(i)}$ indicate the number of ligands X(*i*) surrounding A(*i*), B(*i*) and M(*i*), respectively, while $N_{X(i)-A(i)}$, $N_{X(i)-B(i)}$ and $N_{X(i)-M(i)}$ indicate the number of cations A(*i*), B(*i*) and M(*i*) surrounding ligands X(*i*), respectively. $N_{x(i)}$ is the coordination number of atom X(*i*).

In cubic elpasolites $A^I_2B^IM^{III}X_6$ (X = Cl, Br), only one crystal site (*i* = 1) exists for each atom, with *w*(A) = 8, *w*(B) = 4, *w*(M) = 4, *w*(X) = 24 and *Z* = 4. $N_{A-X} = 12 = N_A$, $N_{B-X} = 6 = N_B$, $N_{M-X} = 6 = N_M$, $N_{X-A} = 4$, $N_{X-B} = 1$ and $N_{X-M} = 1$, so $N_x = 6$. The compound is then decomposed as $(A_2X_4)(B_1X_1)(M_1X_1)$. In this simple situation, Eqn. (2) becomes $he = (6f_c \propto Q_X^2)^{1/2}$ for site M. Q_X, the effective charge carried by ligands X in each binary unit M_mX_x is calculated as $Q_X = \frac{m}{x}Q_M$, where Q_M is the effective charge of the considered cation M, taken here as its bond valence sum (BVS). The calculation of the fractional covalency and volume polarization of individual bond is described elsewhere [24-29] and not reproduced here. A lab-scale calculator was designed [30] in this purpose. The input data are the cation-ligand distances within all coordination polyhedra, the unit cell volume and the cations bond valence sums. These quantities are easily obtained from the crystal structure of the host lattice using e.g. VESTA software [31]. The necessary values of bond valence parameters are picked up in [32]. In the present case, Sb^{3+} and Bi^{3+} doping occurs

at the octahedrally coordinated M^{III} sites of the elpasolite structure. This creates a local distortion due to ionic radii mismatches that alters the M-X distances following $d_{D-X} = d_{M-X} - ½ [r_6(D) – r_6(M)]$ where D designates the dopant Sb^{3+} or Bi^{3+}. The ionic radii $r_6(D)$ and $r_6(M)$ in six-fold coordination are picked up in [33]. These corrected distances are used as input data for the calculation of *he*.

3. Results and discussion

3.1. Excitation of the luminescence

Table 1 collects the experimental position $E_{A,exp}$ of the A excitation of Sb^{3+} and Bi^{3+} in some DHPs and other halides. When the A excitation is splitted by the action of a Jahn-Teller effect, the position of the two maxima is given and the average energy appears in brackets. In the oxi-halides A_2InX_5, H_2O (A = Cs,Rb ; X = Cl,Rb), the *he* value is affected by the presence of an oxygen atom in the first coordination neighbourhood of the doping site and is calculated accordingly.

Table 1. Structural and spectroscopic data related to Sb^{3+} or Bi^{3+}-doped halides : crystal database (ICSD: Inorganic Crystal Structure Database, MP:Materials Project), BVS : bond valence sum pertaining to the cation subtituted by dopant D = Sb^{3+} or Bi^{3+}, *he* : nephelauxetic function at the lattice doping site, $E_{A,exp}$: experimental position of the A excitation, $E_{A,\ calc}$: calculated values of the A excitation using Eqn. (5) and (K,n) coefficient (see text and Fig. 2). Energies in eV.

Compound	Crystal database	BVS	*he*	m’	$E_{A,\ exp.}$	$E_{A,\ calc.}$	Ref
D = Sb³⁺	*free ion*		*0*		*8.27*		15
$SbCl_3$	ICSD-8258	3.11	2.73	0.163	4.59[a]	3.83	17
KCl	ICSD-187219	1.02	1.15	0.388	4.57	4.56	34
NaCl	ICSD-181148	0.98	1.04	0.423	4.63	4.64	35
$Cs_2NaSbCl_6$ (localized)	MP-989514	2.54	2.90	0.187	3.83 + 3.74 (3.78)	3.77	36
$Cs_2NaScCl_6$	MP-1111988	2.82	2.82	0.189	3.90 + 3.78 (3.84)	3.79	37
$Cs_2NaInCl_6$	MP-989571	2.84	2.87	0.188	3.91 + 3.72 (3.81) 3.93 + 3.70 (3.81) 3.987 + 3.70 (3.78)	3.78	3 4 5
Cs_2KInCl_6	MP-1112759	2.89	2.89	0.188	3.86 + 3.66 (3.76)	3.77	5
Rb_3InCl_6 (cubic) Rb_3InCl_6 (monoclinic)	MP-1114625 [11]	2.95 3.15(In1) 3.19(In2)	2.92 2.95 2.96	0.189 0.185 0.185	3.84 + 3.56 (3.70)[a] 3.86 + 3.62 (3.74)	3.76 3.75 3.75	10 11
Cs_3InCl_6	MP-1112991	2.90	2.90	0.185	3.82[a]	3.77	10
Cs_2NaYCl_6	ICSD-245353	3.31	3.21	0.167	3.91 + 3.75 (3.83)	3.67	37
$Cs_2NaLaCl_6$	ICSD-425945	3.56	3.49	0.154	3.91 + 3.75 (3.83)	3.59	37
Cs_2SnCl_6	MP-608555	4.07	4.73	0.126	3.38 + 3.04 (3.21)	3.26	7
Cs_2InCl_5,H_2O	ICSD-63008	2.82	2.63	0.213	3.64	3.86	6
Rb_2InCl_5,H_2O	ICSD-63007	3.39	2.78	0.193	3.83	3.81	10
$SbBr_3$	ICSD-27405	3.17	3.00	0.178	3.84	3.74	17
$Cs_2NaSbBr_6$ (delocalized)	MP-1112142	2.52	3.19	0.202	2.94 (STE)	3.68	36
$Cs_2NaScBr_6$	MP-1112534	2.74	3.08	0.191	3.49 + 3.33 (3.41)	3.71	38
Cs_2NaYBr_6	ICSD-65733	3.35	3.69	0.159	3.47 + 3.33 (3.40)	3.54	38
$Cs_2NaLaBr_6$	ICSD-426112	3.89	4.09	0.144	3.43 + 3.33 (3.38)	3.43	38
Cs_2InBr_5,H_2O	ICSD-130591	3.14	2.96	0.185	3.50	3.69	6
D = Bi³⁺	*free ion*		*0*		*9.41*		15

$BiCl_3$	ICSD-41179	3.37	3.04	0.186	4.09	3.73	17
NaCl	ICSD-181148	0.98	1.17	0.508	3.81	3.81	39
KCl	ICSD-187219	1.02	1.30	0.457	3.70	3.80	39,40
RbCl	ICSD-22166	1.06	1.35	0.467	3.48	3.79	39
$Cs_2AgInCl_6$	ICSD-11524	3.20	3.31	0.193	3.44 3.37	3.72	41 42
$Cs_2NaBiCl_6$ (localized)	ICSD-59195	3.62	3.70	0.164	3.83 + 3.54 (3.69)	3.71	43
Cs_2NaYCl_6	ICSD-245353	3.31	3.52	0.168	3.84	3.71	44
$Cs_2NaLaCl_6$	ICSD-425945	3.62	3.83	0.153	3.90	3.70	45
Cs_2SnCl_6	MP-608555	4.07	5.28	0.118	3.55	3.68	46
$CsMgCl_3$	ICSD-54167	1.94	1.60	0.352	4.37	3.78	47
$BiBr_3$	ICSD-100293	3.22	2.97	0.220	3.25	3.73	17
KBr	ICSD-187220	0.95	1.44	0.443	3.40	3.79	48
Cs_2NaYBr_6	ICSD-65733	3.35	4.33	0.148	3.36	3.69	45
$CsCdBr_3$	ICSD-87261	1.93	1.72	0.345	4.33	3.77	47

[a] indicative

The E_A energies calculated by means of Duffy's equation (Eqn.(1)) are listed in Table 2. We see that they do not match the $E_{A,exp.}$ values of Table 1 very accurately.

Table 2. Energy values of E_A in eV calculated from Eqn. (1).

	D = Sb^{3+} (*m* = 0.24)	D = Bi^{3+} (*m* = 0.28)
Hexa-coordinated chlorides (*h* = 2.0)	4.30	4.14
Hexa-coordinated bromides (*h* = 2.3)	3.70	3.35

In an attempt to improve the situation, we propose to reformulate Duffy's equation as follows :

$$E_A = E_f\ (1 - m'he) \qquad (3)$$

where *m'* relates to the ns^2 cation similarly to *m* in Eqn. (1). The values of *m'* listed in Table 1 are obtained by injecting *he* and $E_{A,exp.}$ in Eqn. (3). In contrast to the *m* values of Duffy, they are found to vary from one lattice to another. This indicates that m' does not depend only upon the cation. Interesting correlations are revealed by Table 1. They are plotted in Fig. 2. First, we find a linear connection between *m'* and BVS, the bond valence sum of the lattice cation that is substituted by Sb^{3+} or Bi^{3+}, and second, we find a power law correlation (solid lines in Fig. 2) between *m'* and *he*, according to :

$$m' = \frac{K}{he^n} \qquad (4)$$

with (K,n) = (0.435 ,0.790) for Sb^{3+} and (0.594,0.985) for Bi^{3+}. This result confirms the earlier observation of Reisfeld and Boehm who concluded on the probable inter-relation between *m* and the nepehlauxetic fonction *h* in Duffy's model [49]. Using Eqn. (4), we reformulate Eqn. (3) as follows :

$$E_A = E_f\ (1 - Khe^{1-n}) \qquad (5)$$

This equation depends now only on the nephelauxetic function *he*, i. e. on the structural characteristics of the host lattice. The corresponding calculated values of E_A are compared to $E_{A,exp.}$ in Table 1. Note that a rough estimation of E_A can be obtained by substituting *he* to BVS in Eqn. (5).

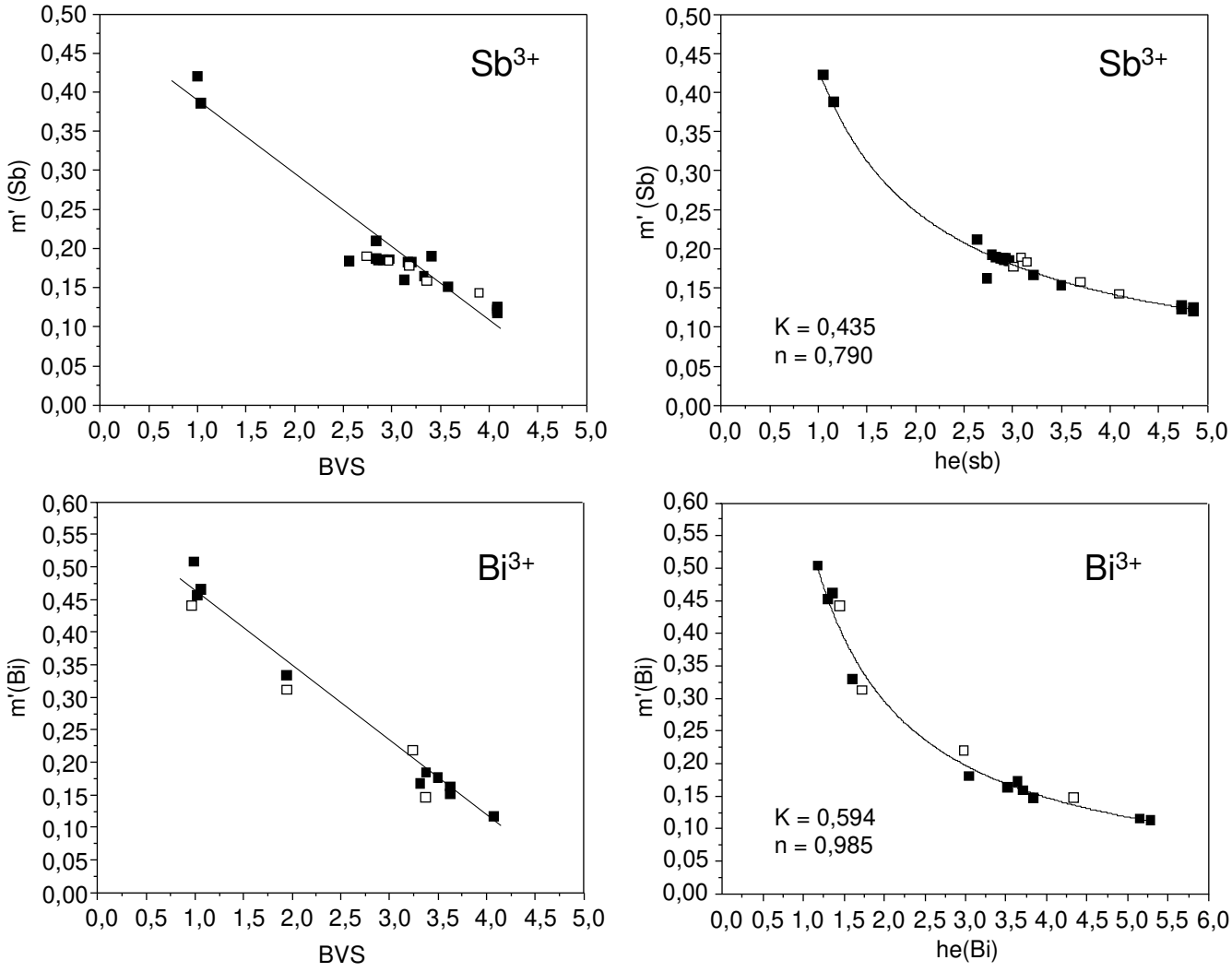

Fig. 2. Variation of *m'* against BVS and *he* for Sb^{3+} and Bi^{3+} in octahedral halide field. Full and empty squares relate to chlorides and bromides, respectively. The solid lines and parameters (K,n) result from fitting, see text for details.

The model looks meaningful and discriminates well the behavior of localized and delocalized states, as examplified by $Cs_2NaSbCl_6$ (localized state) that is well predicted and $Cs_2NaSbBr_6$ (delocalized state) that is not (and should not !) [36]. This holds for stoichiometric Sb or Bi halides. The model, however, fails in predicting the A position of Bi^{3+}-doped $CsCdCl_3$ and $CsMgBr_3$ but we note that for these two compounds, G. Blasse concluded in [47] that « the Bi^{3+} ion in $CsCdBr_3$ and $CsMgCl_3$ is charge-compensated in a special way and that it is impossible to specify the nature of the optical transitions involved in any detail».

3.2. Emission

Let us concentrate now on the Stokes shift (*ΔS*) pertaining to the $^3T_{1u}$ ($^3P_1$) → $^1A_{1g}$ ($^1S_0$) emission of Sb^{3+} in DHPs. The values of ΔS given in Table 3 are taken as the difference between the maximum of the lowest excitation component and the maximum of the emission of Sb^{3+} in the cesium sodo-elpasolites Cs_2NaMX_6 (M = Sc, In, Y, Sb, La ; X = Cl, Br). All the compounds listed in this Table show a dynamical JT splitting of their A excitation but only one emission band. This indicates that the JT splitting does not generate two different minima on the $^3T_{1u}$ APES. G. Blasse et al. suggested that emission emerges from a tetragonal minimum on the APES of the $^3T_{1u}$ relaxed excited state [37,38].

Table 3 - Values of Stokes shifts ΔS associated with $5s^1p^1 \rightarrow 5s^2$ emission of Sb^{3+} in cesium sodo-elpasolites Cs_2NaMX_6 (M = Sc, In, Y, Sb, La ; X = Cl, Br). $\hbar\omega$ pertains to the vibration modes of an ideal quasi-molecular $(SbX_6)^{3-}$ octahedron and μ is its corresponding reduced mass.

Compound	r_6(M) – r_6(Sb) (Å)	$\hbar\omega$ (meV / cm^{-1}) - ω ($10^{13}s^{-1}$)	μ (10^{-25} kg)	ΔS (eV)	Ref
$Cs_2NaScCl_6$	-0.015	33.1 / 267 – 5.03 (A_{1g}) 26.5 / 214 – 4.02 (E_g) 13.7 / 111 – 2.08 (T_{2g})	1.85	0.90	37
$Cs_2NaInCl_6$	0.040			0.93	3-5
Cs_2NaYCl_6	0.140			1.10	37
$Cs_2NaSbCl_6$	0.170*			1.11 (LT)	36
$Cs_2NaLaCl_6$	0.272			1.24	37
$Cs_2NaScBr_6$	-0.015	22.3 / 180 – 3.39 (A_{1g}) 19.0 / 153 – 2.89 (E_g) 9.0 / 73 – 1.37 (T_{2g})	3.33	0.80	38
Cs_2NaYBr_6	0.140			0.90	38
$Cs_2NaLaBr_6$	0.272			1.11	38

* based on an ionic radius of 0.93 Å for Sb^{3+} [50]. LT : low temperature

In first intention, we treat the Stokes shift as $\Delta S = 2S\hbar\omega(A_{1g})\Delta r^2$ with $\hbar\omega(A_{1g})$ the energy of the symmetric A_{1g} breathing mode of the ideal quasi molecular $(SbX_6)^{3-}$ octahedron (X = Cl, Br) and $S = \frac{\mu}{2\hbar}\omega(A_{1g})$ the Huang-Rhys factor, where μ is the reduced mass of the octahedron. This quantity is calculated as $I(SbX_6)/d_{Sb-X}^2$ where $I(SbX_6)$ is the mass moment inertia of the $(SbX_6)^{3-}$ octahedron and d_{Sb-X} is the distance separating Sb and X. Values are given in Table 3. The $\hbar\omega$ vibrational energies listed in Table 3 are assumed being representative of the ideal quasi molecular $(SbX_6)^{3-}$ octahedron [51,52]. Following G. Blasse and A. Bril [19], Δr is the difference of larger outer orbital radius connected with 5s ground state (0.97 Å) and 5p excited state (1.16 Å) of Sb^{3+}, as derived from Waber and Cromer calculations [53]. In first approximation, this quantity (≈ 0.19 Å) is considered as a measure of the difference between the values of equilibrium distance of the ground and excited states of Sb^{3+}. In this macroscopic frame, we arrive to Stokes shifts of 1.05 eV and 0.86 eV for the ideal $(SbCl_6)^{3-}$ and $(SbBr_6)^{3-}$ octahedron, respectively. These values compare quite well those of cesium sodo-elpasolites and suggest that the approximations made above are acceptable, in first intention, for these compounds. This, however, can be improved somehow if we consider the difference in ionic radius r_6(M) – r_6(Sb) between Sb^{3+} and its doping site in the lattice octahedron. In this aim, we show in Fig. 3 the variation of ΔS against r_6(M) – r_6(Sb).

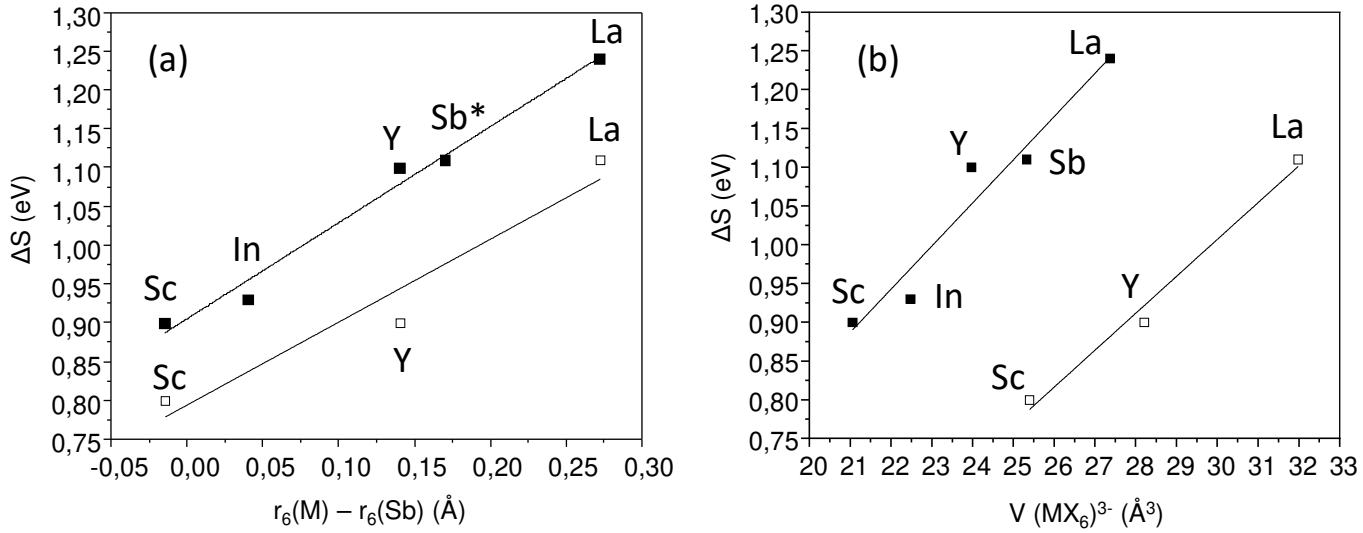

Fig. 3. Variation of ΔS and against r_6(M) – r_6(Sb) (a) and against the $(MX_6)^{3-}$ octahedron volume (b) in Sb^{3+}-doped Cs_2NaMX_6 (M = Sc, In, Y, Sb, La ; X = Cl, Br). Full squares relate to chloro-elpasolites and empty squares relate to bromo-elpasolites. * : r_6(Sb) value from [50].

In line with George Blasse's intuition [37,38,54], the variation is linear and obeys $\Delta S = 0.905 + 1.238\,[r_6(M) - r_6(Sb)]$ for the chloro-elpasolites and $\Delta S = 0.795 + 1.067\,[r_6(M) - r_6(Sb)]$ for the bromo-elpasolites. Fig. 3 reveals the same trend by plotting ΔS against the $(MX_6)^{3-}$ octahedron volume, as formalized by $\Delta S = 0.905 + 0.0557\,[V(MCl_6)^{3-} - 21.33]$ and $\Delta S = 0.795 + 0.0476\,[V(MBr_6)^{3-} - 25.52]$ for chloro- and bromo-elpasolites, respectively. The values in correspondence with $r_6(M) = r_6(Sb)$ are viewed as the Stokes shift of the ideal $(SbX_6)^{3-}$ octahedron in cesium sodo-elpasolites, i. e. not constrained as in Cs_2NaScX_6 or expanded as in the other elpasolites. The corresponding ideal octahedron volume is 21.33 Å^3 for $(SbCl_6)^{3-}$ or 25.52 Å^3 for $(SbBr_6)^{3-}$, as it appears in the equations above. The associated vibration quantum $\hbar\omega$, as calculated from the above equations, amounts 30.6 meV (247 cm^{-1}) for $(SbCl_6)^{3-}$ and 21.4 meV (172 cm^{-1}) for $(SbBr_6)^{3-}$. This quantum is percieved as a combination of the modes, most probably A_{1g} and E_g, that are involved in the lattice relaxation.

Now, we find that increasing the mass of atom B^I in the DHPs affects the Stokes shift of the Sb^{3+} emission quite significantly. A few examples are listed in Table 4. As regard to their large ΔS values, the emission in these compounds is sometimes ascribed to self-trapped excitons in the recent literature, but the concept behind and the related luminescence mechanism are not totally clear. Emission with excitonic character has been demonstrated for Sb^{3+} and Bi^{3+} in oxidic media [55-58]; it involves the transfer of an electron from the ns^2 dopant to the closest-lying lattice cation and subsequent formation of an exciton trapped at the dopant site. This trapped exciton emits usually with a large Stokes shift. However, this process is compromised in the Sb^{3+}-doped DHP elpasolites owing to the large distance (≈7 Å or more) separating the electron donor (Sb^{3+}) to the closest electron acceptor (In^{3+}) in the lattices. As we show in Table 1, the excitation of the luminescence in the Sb^{3+}-doped DHPs is more probably of intraionic $5s^2$ (A_{1g}) → $5s^1p^1$ ($^3T_{1u}$) origin. Unless the excitation energy is transferred to another activator, we should consider that $^3T_{1u}$ is the emitting level at room temperature in these compounds.

Table 4 Stokes shifts, volume and reduced mass of $(InCl_6)^{3-}$and $(B^ICl_6)^{5-}$ octahedra in some Sb^{3+}-doped chloro DP indates.

Compound	ΔS (eV)	V $(InCl_6)^{3-}$ (Å^3)	V $(B^ICl_6)^{5-}$ (Å^3)	μ $(B^ICl_6)^{5-}$ (10^{-25} kg)	Ref
$Cs_2NaInCl_6$	0.93	22.28	29.92	1.303	3-5
Cs_2KInCl_6	1.26	22.11	37.02	1.392	5
Cs_3InCl_6	1.38	22.09	46.46	1.911	10

Among the Sb^{3+}-doped chloro-DP indates listed in Table 4, only $Cs_2NaInCl_6$ has its Stokes shift reproduced by the above equations. We note that the $(InCl_6)^{3-}$ volume is similar for all and close to the ideal value of 21.33 Å. This confirms the quasi-molecular character of the $(MCl_6)^{3-}$ octahedron in these DPs. The greatest change is that of the $(B^ICl_6)^{5-}$ octahedron. Since these octahedra share corners with $(In(Sb)Cl_6)^{3-}$ (See Fig. 1), any change in their mass (and related volume) has consequences on the Stokes shift of the $(SbCl_6)^{3-}$ emission. This is depicted in Fig. 4 and reproduced with $\Delta S = 0.905 + 0.0264\,[V(B^ICl_6)^{5-} - 27.05]$.

Compiling the equations, we empirically approximate the Stokes shift of Sb^{3+} in $Cs_2B^IMCl_6$ (B^I = Na, K, Cs ; M = Sc, In, Y, Sb, La) as :

$$\Delta S = 0.905 + 0.0557\,V(MCl_6)^{3-} + 0.0264\,V(B^ICl_6)^{5-} - 1.902 \qquad (6)$$

where $V(MCl_6)^{3-}$ and $V(B^ICl_6)^{5-}$ represent the volume (in Å^3) of the octahedra. The accuracy is found better than ± 0.1 eV.

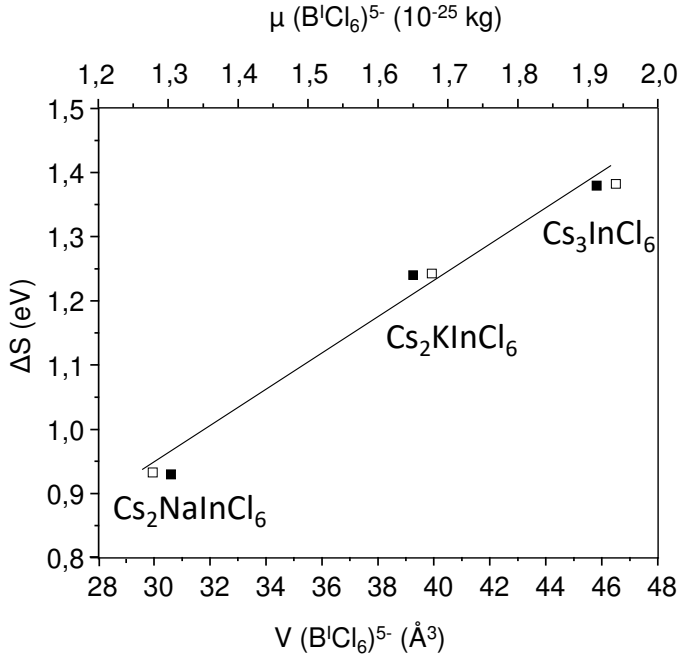

Fig. 4. The Stokes shift associated with $(SbCl_6)^{3-}$ emission against the volume (full squares, lower scale) and reduced mass (empty squares, upper scale) of $(B^{I}Cl_6)^{5-}$ octahedra in some Sb^{3+}-doped chloro DP indates.

At this stage, additional data are needed to go further in the rationalization and generalize the method to any composition of Sb^{3+}-doped DHP. The chemistry of this family of compounds is however so rich that a prospection based on trial-error or combinational chemistry is no longer adequate. Machine learning (ML) strategies may solve the problem, subject that appropriate descriptors are implemented in the algorithms. Equations (5) and (6) published in this paper emerge as possible structure-property descriptors to start the ML procedure. This would typically involve :

(1) data mining, i. e. screening of appropriate combinations of atoms to form $A^{I}_2B^{I}M^{III}X_6$ DPs, evaluation of the thermodynamic phase stability of the so-formed compound and corresponding structural properties. This step would typically use crystal or materials databases (Crystallography Open Database, Inorganic Crystal Structure Database, Materials Project, Springer Materials, Materials Platform for Data Science, …) or involve calculations based on DFT theory (Materials Studio, Vienna Ab Initio Simulation Package, …) [24,25, 59]

(2) extraction of the necessary structural parameters and calculation of *he* to run the equations and predict the position of the excitation and emission bands. The synthesis and optical characterization of some relevant chemical compositions could then enrich the spectroscopic database and contribute to refine the existing descriptor in an auto-adaptative manner. Note that this preliminary methodology holds for intra-ionic $5s^2 \leftrightarrow 5s^1p^1$ transitions of quasi-molecular Sb^{3+} in halide octahedral fields, in the macroscopic approximation of symmetric breathing. This, however, does not allow reproducing the properties of a compound like $Cs_2SnCl_6:Sb^{3+}$ that shows two emission bands instead of a single one. The intensity of these two bands vary strongly with temperature as a consequence of a possible JT perturbation [7] similar to that reported by G. Blasse et. al in $LnPO_4:Sb^{3+}$ (Ln=Sc, Lu, Y) [60,61]. In $Cs_2SnCl_6:Sb^{3+}$, we do not exclude that charge compensation plays a critical role. This question needs to be worked out for further rationalization.

4. Conclusion

The model introduced by J. A. Duffy to locate the position of A excitation band in ns^2-doped solids is reformulated for Sb^{3+} and Bi^{3+} in double halide perovskites by substituting the lattice-related nephelauxetic function *h* to a more

accurate fonction, *he*, computable from crystal structure data. Concomitantly, the ns^2 cation-related *m* parameter in Duffy's model is substituted to parameter *m',* whose value shows a power law correlation with *he*. This *m' - he* inter-relation is rationalized in the form of a new equation allowing to calculate the energy of the A band only from the knowledge of the DHPs' crystal structure. The Stokes shifts pertaining to the $5s^1p^1$ ($^3T_{1u}$) → $5s^2$ (A_{1g}) emission of Sb^{3+} in « 0D » cubic elpasolites is macroscopically rationalized in the approximation of a symmetrically breathing quasi-molecular $(SbX_6)^{3-}$ octahedron (X = Cl, Br). The so-obtained preliminary results have possible interest as descriptors for further computer-assisted design of double halide perovskites doped with Sb^{3+}.

Declaration of competing interest

The author have no competing interests to declare

Sample CRediT author statement

Philippe Boutinaud : Conceptualization; Formal analysis; Investigation; Methodology; Writing & editing.

Caption for figures

Fig. 1 View of the $A^{I}_2B^{I}M^{III}X_6$ double perovskite structure.

Fig. 2. Variation of *m'* against BVS and *he* for Sb^{3+} and Bi^{3+} in octahedral halide field. Full and empty squares relate to chlorides and bromides, respectively. The solid lines and parameters (K,n) result from fitting, see text for details.

Fig. 3. Variation of *ΔS* and against $r_6(M) - r_6(Sb)$ (a) and against the $(MX_6)^{3-}$ octahedron volume (b) in Sb^{3+}-doped Cs_2NaMX_6 (M = Sc, In, Y, Sb, La ; X = Cl, Br). Full squares relate to chloro-elpasolites and empty squares relate to bromo-elpasolites. * : value from [50].

Fig. 4. The Stokes shift associated with $(SbCl_6)^{3-}$ emission against the volume (full squares, lower scale) and reduced mass (empty squares, upper scale) of $(B^{I}Cl_6)^{5-}$ octahedra in some Sb^{3+}-doped chloro DP indates.

References

[1] G. Blasse, Classical phosphors : a Pandora's box, J. Lumin. 72-74 (1997) 129-134. https://doi.org/10.1016/S0022-2313(96)00166-4

[2] A. H. McKeag, P. W. Randy (1949) US Patent 2,448,733

[3] M. B. Gray, S. Hariyani, T. A. Strom, J. D. Majher, J. Brgoch, P. M. Woodward, High-efficiency blue photoluminescence in the $Cs_2NaInCl_6$:Sb^{3+} double perovskite phosphor, J. Mater. Chem. C 8 (2020) 6797 – 6803. https://doi.org/10.1039/D0TC01037E

[4] R. Zeng, L. Zhang, Y. Xue, B. Ke, Z. Zhao, D. Huang, Q. Wei, W. Zhou and B. Zou, Highly Efficient Blue Emission from Self-Trapped Excitons in Stable Sb^{3+}-Doped $Cs_2NaInCl_6$ Double Perovskites, J. Phys. Chem. Lett. 11 (2020) 2053 - 2061. https://doi.org/10.1021/acs.jpclett.0c00330

[5] A. Noculak, V. Morad, K. M. McCall, S. Yakunin, Y. Shynkarenko, M. Wörle, M. V. Kovalenko, Bright Blue and Green Luminescence of Sb(III) in Double Perovskite Cs_2MInCl_6 (M = Na, K) Matrices, Chem. Mater. 32 (2020) 5118−5124. https://doi.org/10.1021/acs.chemmater.0c01004

[6] Y. Jing, Y. Liu, X. Jiang, M. S. Molokeev, Z. Lin, Z. Xia, Sb^{3+} Dopant and Halogen Substitution Triggered Highly Efficient and Tunable Emission in Lead-Free Metal Halide Single Crystals, Chem. Mater. 32 (2020) 5327−5334. https://doi.org/10.1021/acs.chemmater.0c01708

[7] J. Li, Z. Tan, M. Hu, C. Chen, J. Luo, S. Li, L. Gao, Z. Xiao, G. Niu, J. Tang, Antimony doped Cs_2SnCl_6 with bright and stable emission, Front. Optoelectron. 12 (2019) 352–364. https://doi.org/10.1007/s12200-019-0907-4

[8] Y. Jing, Y. Liu, J. Zhao and Z. Xia, Sb^{3+} Doping-Induced Triplet Self-Trapped Excitons Emission in Lead-Free Cs_2SnCl_6 Nanocrystals, J. Phys. Chem. Lett. 10 (2019) 7439 - 7444. https://doi.org/10.1021/acs.jpclett.9b03035

[9] S. Wu, W. Li, J. Hu, P. Gao, Antimony doped lead-free double perovskites ($Cs_2NaBi_{1-x}Sb_xCl_6$) with enhanced light absorption and tunable emission, J. Mater. Chem. C 8 (2020) 13603 – 13611. https://doi.org/10.1039/D0TC03003A

[10] P. Han, C. Luo, S. Yang, Y. Yang, W. Deng, K. Han, All-Inorganic Lead-free 0D perovskites by a doping strategy to achieve a PLQY boost from <2% to 90%, Angew. Chem. Int. Ed. 59 (2020) 12709–12713. https://doi.org/10.1002/anie.202003234

[11] J. D. Majher, M. B. Gray, T. Liu, N. P. Holzapfel, P. M. Woodward, Rb_3InCl_6: a monoclinic double perovskite derivative with bright Sb^{3+}-activated photoluminescence, Inorg. Chem. 59 (2020) 14478−14485. https://doi.org/10.1021/acs.inorgchem.0c02248

[12] P. W. M. Jacobs, Alkali halide crystals containing impurity ions with the ns^2 ground-state electronic configuration, J. Phys. Chem. Solids 52 (1991) 35-67. https://doi.org/10.1016/0022-3697(91)90059-9

[13] J.A. Duffy, M.D. Ingram, New correlation between s-p spectra and the nephelauxetic ratio *β*: applications in molten salt and glass chemistry, J. Chem. Phys. 54 (1971) 443–444. https://doi.org/10.1063/1.1674635

[14] A. Duffy, Prediction of ultraviolet absorption spectra of p-block ions in oxide media. Possible application to redox equilibria in glasses and molten salts, J. Chem. Soc., Faraday Trans. 2, 74 (1978) 1504-1514. https://doi.org/10.1039/F29787401504

[15] C.E. Moore, *Atomic Energy Levels,* National Bureau of Standards, Washington, DC, 1952

[16] C.K. Jørgensen, Absorption Spectra and Chemical Bonding in Complexes, Pergamon Press, Oxford, 1962

[17] A. J. Bruce, J. A. Duffy, Thin films absorption spectra of lower valent p block halides, Thin Solid Films 101 (1983) 179-192. https://doi.org/10.1016/0040-6090(83)90269-9

[18] A. Duffy, M.D. Ingram, Use of thallium(I), lead(II), and bismuth(III) as spectroscopic probes for ionic–covalent interaction in glasses, J. Chem. Phys. 52 (1970) 3752–3754. https://doi.org/10.1063/1.1673553

[19] G. Blasse, A. Bril, Photoluminescent efficiency of phosphors with electronic transitions in localized centers, J. Electrochem. Soc. : Solid State Science 115 (1968) 1067-1075. https://doi.org/10.1149/1.2410880

[20] J. Schmidt, J. Shi, P. Borlido, L. Chen, S. Botti, M. A. L. Marques, Predicting the thermodynamic stability of solids combining density functional theory and machine learning, Chem. Mater. 29 (2017) 5090-5103. https://doi.org/10.1021/acs.chemmater.7b00156

[21] Q. Tao, P. Xu, M. Li, W. Lu, Machine learning for perovkite materials design and discovery, npj Computational Materials 7 (2021) 23. https://doi.org/10.1038/s41524-021-00495-8
[22] J. S. Shi, S. Y. Zhang, Barycenter of Energy of Lanthanide $4f^{N-1}5d$ Configuration in Inorganic Crystals, J. Phys. Chem. B 108 (2004) 18845-18849. https://doi.org/10.1021/jp038001b
[23] S. Y. Zhang, F. M. Gao, C. X. Wu, Chemical bond properties of rare earth ions in crystals, J. Alloys Compds 275-277 (1998) 835-837. https://doi.org/10.1016/S0925-8388(98)00452-6
[24] J. C. Phillips, Dielectric Definition of Electronegativity, Phys. Rev. Lett. 20 (1968) 550-553. https://doi.org/10.1103/PhysRevLett.20.550
[25] J. C. Phillips, Ionicity of the Chemical Bond in Crystals, Rev. Mod. Phys. 42 (1970) 317-356. https://doi.org/10.1103/RevModPhys.42.317
[26] J. A. Van Vechten, Quantum Dielectric Theory of Electronegativity in Covalent Systems. I. Electronic Dielectric Constant, Phys. Rev. 182 (1969) 891- 905. https://doi.org/10.1103/PhysRev.182.891
[27] J. A. Van Vechten, Quantum Dielectric Theory of Electronegativity in Covalent Systems. II. Ionization Potentials and Interband Transition Energies, Phys. Rev. 187 (1969) 1007- 1020. https://doi.org/10.1103/PhysRev.187.1007
[28] B. F. Levine, d-Electron Effects on Bond Susceptibilities and Ionicities, Phys. Rev. B 7 (1973) 2591- 2600. https://doi.org/10.1103/PhysRevB.7.2591
[29] F. Gao, S. Zhang, Investigation of mechanism of nephelauxetic effect, J. Phys. Chem. Solids 58 (1997) 1991-1994. https://doi.org/10.1016/S0022-3697(96)00139-4
[30] M. Amer, PhD Thesis n° 935, Clermont-Ferrand, Dec. 2017
[31] K. Momma, F. Izumi, - VESTA: a three-dimensional visualization system for electronic and structural analysis, J. Appl. Crystallogr. 41 (2008) 653- 658. https://doi.org/10.1107/S0021889808012016
[32] N. E. Breese, M. O'Keefe, Bond-valence parameters for solids, Acta Cryst. B47 (1991) 192-197. https://doi.org/10.1107/S0108768190011041
[33] R. D. Shannon, Revised effective ionic radii and systematic studies of interatomic distances in halides and chalcogenides, Acta Cryst. A32 (1976) 751-767. https://doi.org/10.1107/S0567739476001551
[34] T. Tsuboi, P. Ahmett, J. G. Kang, Optical absorption bands due to the $s^2 \rightarrow$ sp transition in KCl :Sb^{3+} crystals, J. Phys.: Condens. Matter 4 (1992) 531-534. https://doi.org/10.1088/0953-8984/4/2/020
[35] S. Radhakrishna, A. M. Karguppikar, Defect centers in antimony doped NaCl crystals, J. Phys. Chem. Solids 34 (1973) 1497-1505. https://doi.org/10.1016/S0022-3697(73)80222-7
[36] - E. W. J. L. Oomen, W. M. Smit, G. Blasse, Luminescence of $Cs_2NaSbCl_6$ and $Cs_2NaSbBr_6$: a transition from a localized to a delocalized excited state, Chem. Phys. Lett. 138 (1987) 23-28. https://doi.org/10.1016/0009-2614(87)80336-6
[37] E. W. J. L. Oomen, W. M. Smit, G. Blasse, On the luminescence of Sb^{3+} in Cs_2NaMCl_6 (with M = Sc,Y,La) : a model system for the study of trivalent s^2 ions, J. Phys. C : Solid state Phys. 19 (1986) 3263-3272. https://doi.org/10.1088/0022-3719/19/17/020
[38] E. W. J. L. Oomen, G. J. Dirksen, W. M. Smit, G. Blasse, On the luminescence of the Sb^{3+} ion in Cs_2NaMBr_6 (M = Sc,Y,La), J. Phys. C : Solid state Phys. 20 (1987) 1161-1171. https://doi.org/10.1088/0022-3719/20/8/017
[39] S. Radhakrishna, R. Setty, Bismuth centers in alkali halides, Phys. Rev. 14 (1976) 969-976. https://doi.org/10.1103/PhysRevB.14.969
[40] J. G. Kang, H. M. Yoon, G. M. Chun, Y. D. Kim, T. Tsuboi, Spectroscopic studies of Bi^{3+} colour centres in KCl single crystals, J. Phys.: Condens. Matter 6 (1994) 2101-2116. https://doi.org/10.1088/0953-8984/6/10/028
[41] M. B. Gray, J. D. Majher, T. A. Strom, P. M. Woodward, Broadband white emission in $Cs_2AgIn_{1-x}Bi_xCl_6$ phosphors, Inorg. Chem. 58 (2019) 13403-13410. https://doi.org/10.1021/acs.inorgchem.9b02299
[42] Y. Liu, Y. Jing, J. Zhao, Q. Liu, Z. Xia, Design optimization of lead-free perovskite $Cs_2AgInCl_6$:Bi nanocrystals with 11.4% photoluminescence quantum yield, Chem. Mater. 31 (2019) 3333−3339. https://doi.org/10.1021/acs.chemmater.9b00410
[43] F. Pelle, B. Jacquier, J.P. Denis and B. Blanzat, Optical properties of $Cs_2NaBiCl_6$, J. Luminescence 17 (1978) 61-72. https://doi.org/10.1016/0022-2313(78)90026-1

[44] A.C. van der Steen, Luminescence of Cs_2NaYCl_6-Bi^{3+} ($6s^2$). Phys. Status. Solidi B 100 (1980) 603–611. https://doi.org/10.1002/pssb.2221000227
[45] A. Wolfert, G. Blasse, Luminescence of Bi^{3+}-doped crystals of Cs_2NaYBr_6 and $Cs_2NaLaCl_6$, J. Solid State Chem. 59 (1985) 133–142. https://doi.org/10.1016/0022-4596(85)90310-X
[46] Z. Tan, J. Li, C. Zhang, Z. Li, Q. Hu, Z. Xiao, T. Kamiya, H. Hosono, G. Niu, E. Lifshitz, Y. Cheng and J. Tang, Highly Efficient Blue-Emitting Bi-Doped Cs_2SnCl_6 Perovskite Variant: Photoluminescence Induced by Impurity Doping, Adv. Funct. Mater. 28 (2018) 1801131. https://doi.org/10.1002/adfm.201801131
[47] A. Wolfert, G. Blasse, Luminescence of s^2 Ions in $CsCdBr_3$ and $CsMgCl_3$, J. Solid State Chem. 55 (1984) 344-352. https://doi.org/10.1016/0022-4596(84)90288-3
[48] K. Polak, E. Mihokova, In^+, Pb^{2+} and Bi^{3+} in KBr crystal : luminescence dynamics, Opt. Mater. 32 (2010) 1280-1282. https://doi.org/10.1016/j.optmat.2010.05.006
[49] R. Reisfeld, L. Boehm, The determination of the nephelauxetic effect in oxide glasses by Sn^{2+}, Sb^{3+}, Tl^+, Pb^{2+} and Bi^{3+} ions, J. Non-Cryst. Solids 17 (1975) 209-214. https://doi.org/10.1016/0022-3093(75)90051-4
[50] W. M. A. Smit, G. J. Dirksen**,** D. J. Stufkens, Infrared and Raman spectra of the elpasolites $Cs_2NaSbCl_6$ and $Cs_2NaBiCl_6$: evidence for a pseudo Jahn-Teller distorted ground state, J. Phys. Chem. Solids 51 (1990) 189-196. https://doi.org/10.1016/0022-3697(90)90092-T
[51] T. Barrowcliffe, I. R. Beattie, P. Day, K. Livingstone, The vibrational spectra of some chloro-anions, J. Chem. Soc. (A) (1967) 1810-1812. https://doi.org/10.1039/J19670001810
[52] M. A. Hooper, D. W. James, Vibrational spectra of some Group Vb halides. III. A far-infrared and Raman spectral study of some Hexahalogeno-, Pentahalogeno-, and Tetrahalogeno-bismuthate(III) and -antimonate(III) salts, Austral. J. Chem. 26 (1973) 1401-1412. https://doi.org/10.1071/CH9731401
[53] J. T. Waber, D. T. Cromer, Orbital Radii of Atoms and Ions, J. Chem. Phys. 42 (1965) 4116. https://doi.org/10.1063/1.1695904
[54] E. W. J. L. Oomen, W. M. Smit, G. Blasse, The luminescence of arsenic (III) in the cubic elpasolite $Cs_2NaScCl_6$, Chem. Phys. Lett. 138 (1987) 584-586. https://doi.org/10.1016/0009-2614(87)80129-X
[55] P. Boutinaud, Luminescence of Sb^{3+} in closed shell transition metal oxides, J. Lumin. 208 (2019) 394-401. https://doi.org/10.1016/j.jlumin.2019.01.003
[56] P. Boutinaud, Revisiting the spectroscopy of the Bi^{3+} ion in oxide compounds, Inorg. Chem. 52 (2013) 6028-6038. https://doi.org/10.1021/ic400382k
[57] P. Boutinaud, On the spectroscopy of Bi^{3+} in d^{10} post-transition metal oxides, J. Lumin. 223 (2020) 117219. https://doi.org/10.1016/j.jlumin.2020.117219
[58] A. Krasnikov, E. Mihokova, M. Nikl, S. Zazubovich, Y. Zhydachevskyy, Luminescence spetroscopy and origin of luminescence centers in Bi-doped materials, Crystals 10 (2020) 208. https://doi.org/10.3390/cryst10030208
[59] S. Li, R.-J. Xie, Review-Data driven discovery of novel phosphors, ECS J. Solid State Sci. Technol. 6 (2020) 016013. https://doi.org/10.1149/2.0192001JSS
[60] E.W.J.L. Oomen, W.M.A. Smit, G. Blasse, Jahn-Teller effect in the emission and excitation spectra of the Sb^{3+} ion in LPO_4 (L = Sc, Ln, Y), Phys. Rev. 37 (1988) 18–26. https://doi.org/10.1103/PhysRevB.37.18
[61] E.W.J.L. Oomen, W.M.A. Smit, G. Blasse, Jahn-Teller effect in the Sb^{3+} emission in zircon structured phosphates, Chem. Phys. Lett., 112 (1984) 547-550. https://doi.org/10.1016/0009-2614(84)85775-9